Reflectance Spectrum Based Classification of Ore

Janne Pietilä * **Olli Haavisto** *

* *Helsinki University of Technology (TKK), Department of Automation and Systems Technology, P.O.Box 5500, FI-02015 TKK, Finland (e-mail: janne.pietila@tkk.fi, olli.haavisto@tkk.fi).*

Abstract: The visible and near infrared reflectance spectra of rock samples from a zinc-copper mine are analyzed by data-based multivariate methods. The effect of data preprocessing to the feature extraction of the spectra is discussed. Based on the measurement data, a classification model is developed to automatically separate gangue rocks from ore. The model is detected to classify rock samples with good accuracy and robustness.

Keywords: optical spectroscopy, classification, statistical analysis, data reduction, discriminant analysis

1. INTRODUCTION

In the mining industry the type and quality of ore naturally varies as ore is extracted from different parts of the mine or the open pit. These variations affect the performance of the concentration process and the ore properties should therefore be measured. The information from this kind of measurement could, for instance, be used as a feedforward signal in controlling the grinding mills or as feedback for evaluating and planning the mining operation.

Automatic ore classification techniques for laboratory or small-scale in situ use have been extensively studied and applied, utilizing such varied methods as laser-induced plasma spectroscopy (LIPS) (Kaski et al. (2003)) or prompt gamma neutron activation analysis (PGNAA) (Borsaru et al. (2006)) among others. More recently the online applications have received more attention. Machine vision is a popular approach, with different geometric, textural and colour properties of the images acting as the basis for classification. The acquired image data has been modelled for example with statistical multivariate methods and support vector machines (Tessier et al. (2007)) or with neural networks (Casali et al. (2001); Singh and Rao (2005)). Also methods based on measurements in the microwave reflectance spectrum (Cutmore et al. (1998)) and of x-ray fluorescence (XRF) (Sokolov et al. (2005)) have been applied in an online fashion. Recently near-infrared (NIR) reflectance spectroscopy has been utilized in a gangue mineral concentration measurement by Goetz et al. (2009).

There are also some commercial applications already on the market. One of them is Metso VisioRock (Guyot et al. (2004)), which relies on simultaneous measurements of ore size distribution, colour and texture information. An expert logic is used to determine the ore class by these measurements. Another one, marketed especially for online bulk material characterization in cement industry, is the Solbas technology by ABB, which utilizes NIR reflectance spectrum measurements.

In this study a method for identifying ore types based on the optical reflectance spectrum in the visible and near infrared (VNIR) area from 400 to 1000 nm is examined. This is done by measuring the spectrum of rock samples consisting of crushed drill cores. Concentrating on the VNIR spectrum allows utilizing conventional digital image sensors in the measuring equipment, making the solution quite affordable. This is not typically the case with the sensors sensitive in other areas of the electromagnetic spectrum, where the cost can often be tenfold. The method presented in this paper is also relatively easy to implement, since the equipment is rather compact and e.g. potentially hazardous radiation sources are not used. The spectrum measurement could also be combined with the ore particle size measurement developed earlier by Kaartinen and Tolonen (2008), which would give information of the size and mass distribution of the different types of ore. This would enable classifying pieces of rock based on their size and type directly from a moving conveyor belt. In this study the conveyor belt measurement application is emulated in a laboratory environment.

The rest of this article is organized as follows: the rock samples, measurement setup and methods used are described in Section 2. The data analysis, modelling and results achieved are covered in Section 3, and conclusions are presented in Section 4.

2. MATERIALS AND METHODS

The rock samples used in this study were provided by the Pyhäsalmi copper, zinc and sulphur mine in central Finland. The ore contains chalcopyrite, sphalerite, pyrrhotite and pyrite, with the main gangue minerals being barite and carbonates. The samples consisted of drill cores taken during regular surveying operations. The elemental and mineral contents of twelve core samples were known. In addition there were two samples representing gangue which had not been analyzed for their contents; their mineral contents are assumed small. The samples and their mineral contents are listed in Table 1, where the class column

Table 1. Mineral contents of the rock samples

Sample	Chalco-pyrite (%)	Sphalerite (%)	Pyrite (%)	Class	Data set
A	0.5	26.6	52.4	ore	E
B	2.5	0.3	68.7	ore	V
C	1.9	0.1	73.2	ore	V
D	1.7	0.1	89.8	ore	E
E	0.8	0.1	50.1	ore	V
F	0.3	0.1	6.8	gangue	V
G	1.0	0.2	92.0	ore	V
H	4.1	0.2	92.0	ore	V
I	4.8	0.4	91.3	ore	E
J	4.2	0.4	81.4	ore	V
K	1.6	0.2	92.0	ore	V
L	1.1	0.1	88.0	ore	V
M	-	-	-	gangue	E
N	-	-	-	gangue	E

indicates whether the sample represents ore or gangue. After initial inspection from the intact drill cores, the samples were crushed to a particle size where individual pieces were no larger than approximately 5 cm in diameter. The crushing was done to introduce planes of fracture to the samples, thus improving the resemblance to rock material typically encountered at a conveyor belt in an actual mining environment.

Based on the mineral contents, samples F, M and N were assigned to the gangue class, and the rest of the samples to the ore class. Accordingly, a matrix of desired responses was composed, in which each row corresponded to one average spectrum from a rock sample, and each column to a class (ore/gangue). The values were 1, if the measurement corresponded to a certain class, and zero otherwise. When calibrating the classification model, the measurements from the samples were divided into an estimation set (E) and a validation set (V), as indicated in Table 1.

2.1 Measurement setup

The spectra were obtained with an imaging spectrophotometer, consisting of a spectrograph (Specim ImSpector V10), an industrial digital camera (Basler A102f), and focusing optics. The device provides spectral measurements along a projected line on the object being measured. The image resolution provided by the camera is 1280 (spatial) by 960 (spectral) pixels, although the spectral resolution provided by the spectrograph is actually lower (5 nm in wavelength, corresponding to $(1000 - 400)/5 = 120$ effective wavelength bins). The camera was connected to a PC via Firewire, and the images were acquired using the MATLAB Image Acquisition toolbox. The wavelength axis of the spectrophotometer was calibrated by measuring the spectrum of a mercury-vapor lamp and matching the characteristic peaks in the spectrum.

The spectra of each rock sample were measured in the following way. The sample was spread to a tray, which was then positioned under the spectrophotometer (Figure 1). The spectrophotometer was mounted to a stand, with the distance to the sample being approximately 28 cm. At this distance the width of the measurement line was 13 cm. The

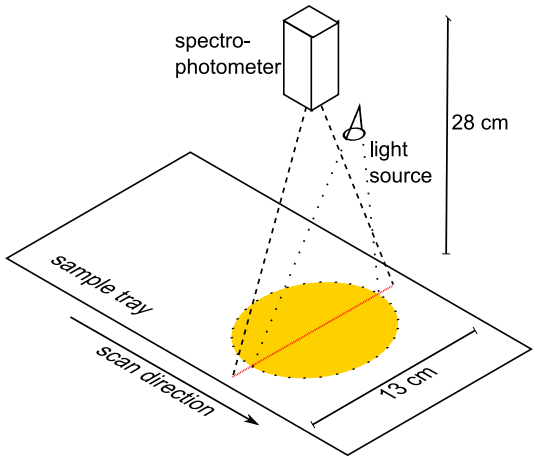

Fig. 1. Schematic of the measurement setup.

sample was illuminated by a single 50 W halogen spotlight (Osram Ministar 50050WFL), which was mounted close to the spectrophotometer to provide unobstructed illumination to the measurement line. The illuminance delivered by this light source was sufficiently high that shielding the measuring station from ambient light was deemed unnecessary (the fluorescent lights in the room were, however, switched off during the measurement). To account for the nonuniform illumination provided by the single light source, a spectral reference image was obtained from a piece of white paper. The average spectrum of the reference image is shown in Figure 2.

A total of 40 960 measurements (32 lines, 1280 spectra/line) were obtained from each rock sample by moving the sample tray in a direction perpendicular to the measurement line between consecutive measurements. Some example spectra from sample D are presented in Figure 2. Measurements from the line ends were discarded due to low intensity values and resulting distortion in the shape of the spectrum. For modelling purposes the average spectrum of each line measurement was calculated from the data. The purpose of this operation was to reduce measurement noise while still preserving some of the variation within samples. Each rock sample was thus represented by 32 average spectra, and since there were 14 rock samples, the total amount of spectra available for modelling was 448.

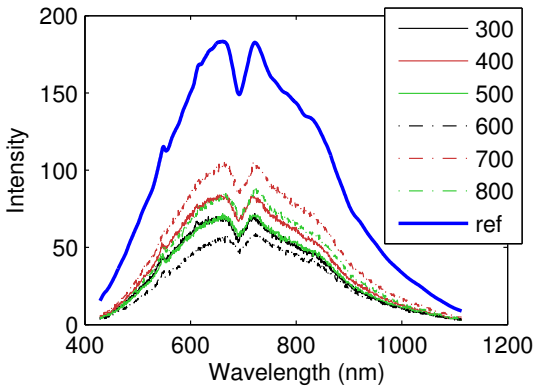

Fig. 2. Average of the white reference and unprocessed spectra from sample D. The legend refers to the position on the measurement line (in pixels).

Of these, 160 data points belonged to the estimation data set and 288 to the validation set.

2.2 Data preprocessing

A good choice of preprocessing can bring out the relevant features of the underlying phenomenon in the data or simplify the model. In the following, the spectrum measurement is denoted by the row vector $\mathbf{x} = [x_1, x_2, \ldots, x_m]$, and the preprocessed measurement by $\tilde{\mathbf{x}}$.

Autoscaling normalizes the variables so that they all have zero mean and unit variance (Burns and Ciurczak (2008)):

$$\tilde{\mathbf{x}} = \mathbf{S}_{\mathbf{x}}^{-1} \left(\mathbf{x} - \mu_{\mathbf{x}} \right), \tag{1}$$

where $\mu_{\mathbf{x}}$ is the mean vector of the spectrum measurement and $\mathbf{S}_{\mathbf{x}} = \mathrm{diag}\left[\sigma_1, \ldots, \sigma_m\right]$ is the matrix of the standard deviations. The result is that all of the preprocessed variables receive equal weighting with the multivariate methods.

First and second derivatives (or differences) can be used to eliminate baseline offsets or trends. The derivative of a spectrum can be defined as

$$\tilde{x}_i = x_{i+1} - x_i, \tag{2}$$

where x_i corresponds to the spectrum intensity at the ith wavelength. Higher order derivatives are obtained by applying the operation multiple times. The derivative is often taken from filtered, e.g. polynomially smoothed, spectra, however this might introduce distortion to the result (Gemperline (2006)).

When reflectance spectra are measured, the result is sometimes transformed according to

$$\tilde{x}_i = -\ln x_i. \tag{3}$$

The intention is to relate the measured reflectance to the absorbance of the sample (Burns and Ciurczak (2008)).

Multiplicative scatter correction (MSC) is used to counter the effects of different particle size distributions (Geladi et al. (1985)). The method uses a linear regression model where each measured spectrum $\mathbf{x}$ is fitted to a reference spectrum $\mathbf{x}_{\mathrm{ref}}$ according to the equation

$$\mathbf{x}_{\mathrm{ref}} = \beta_0 + \beta_1 \mathbf{x}(j) + \varepsilon(j), \tag{4}$$

where β_0 and β_1 are scalar regression coefficients, which are obtained by minimizing the sum of the squared errors $\Sigma_1^N \varepsilon(j)\varepsilon(j)^T$. The reference spectrum is usually selected to be the mean spectrum of the data set. The MSC-corrected spectrum is then calculated by

$$\tilde{\mathbf{x}} = \beta_0 + \beta_1 \mathbf{x}. \tag{5}$$

2.3 Analysis and classification methods

The spectrum measurement used in this study provides a large amount of high-dimensional and mutually correlated data. This kind of data is readily handled by statistical multivariate methods based on latent variables and dimension reduction. Principal component analysis (PCA) is one of the more universal tools of statistical multivariate analysis. PCA reduces the dimension of the data to $k \ll m$ orthogonal directions of variation – principal components – that together explain the maximum amount of variation possible among the original mutually correlated data. The principal component scores $\mathbf{z} = [z_1, \ldots, z_k]$ for a given measurement $\mathbf{x}$ are given by

$$\mathbf{z} = \mathbf{x}\mathbf{F}, \tag{6}$$

where the principal component loadings matrix $\mathbf{F}$ is determined based on the correlations between the original variables, and corresponds to the most prominent features of the spectra. PCA is widely treated in the literature (see e.g. Basilevsky (1994); Jackson (2003)), and specific descriptions related to spectroscopy are also available (Burns and Ciurczak (2008); Gemperline (2006)).

The classification of the ore samples was implemented with partial least squares discriminant analysis (PLS-DA). It is a supervised classification technique, which is based on the PLS regression technique widely used e.g. in NIR calibration (Burns and Ciurczak (2008)). It shares features with the classical linear discriminant analysis (LDA) and has been shown to have better performance in classification than PCA-based discriminant analysis (Barker and Rayens (2003)). In PLS-DA, a linear regression model is constructed on binary response variables, and the technique can be used for multiple classes by assigning a different response variable for each class. The technique utilizes latent variables that are based on the correlation between the measurements and the response variables. The output of the PLS model is compared to a threshold value, which determines the classification. The threshold value is selected based on the distribution of the response variables.

2.4 Validation

Model validation procedures are used to determine the suitable complexity of the model. In crossvalidation a part of the training data set is used to estimate the model parameters and the rest are used to test the model. This process is iterated with different partitioning of the data, usually resulting in each data point having been used for both estimation and validation. If there is a sufficient amount of data points, a subset of these can be dedicated to validation purposes, without ever being used in model estimation. Of course, this is preferable, as the validation data set is completely independent from the training data set, and the validation results are therefore more reliable.

In this study the classification performance was measured by the classification error, i.e. the fraction of misclassifications in the data set, and by the root mean squared error (RMSE) of the model

$$\mathrm{RMSE} = \sqrt{\frac{\sum_1^N \left(\hat{y}(p) - y(p)\right)^2}{N}}, \tag{7}$$

where $\hat{y}(p)$ is the output predicted by the model, $y(p)$ is the actual output value and N is the number of data points. The actual output value is an element of the binary response matrix and therefore has values of either 0 or 1. The output predicted by the model, on the other hand, is a real number and the classification is determined by comparing the model output to a threshold value. The RMSE indicates the capability of the model to separate the classes, as it is based on the difference between the model output (before thresholding) and the desired response. A lower RMSE value indicates larger separation between the classes in the model output.

3. CLASSIFICATION

In this section the data analysis and the development of the classification model are covered. First some specific measurement pretreatment steps for this case are explained. Cluster analysis is carried out with PCA, comparing different preprocessing methods, and then a PLS-DA classification model is developed. Finally, the best classification model is tested with a data set simulating a case that could be encountered on a conveyor belt in an actual process environment.

3.1 Measurement pretreatment

First, the spectral dimension of the measurements was reduced by dividing the spectral wavelength range into L wavelength bins, and calculating the average intensity for each bin. $L = 20$ bins retained sufficient information for classification while significantly reducing the computational load and memory requirements. This reduction in the spectral dimension was done also for the white reference spectra.

The variation due to nonuniform illumination was then eliminated by dividing the intensity of the spectra along the measurement line with the average intensity $\overline{w}_{\text{ref}}$ of the white reference spectra $\mathbf{w}_{\text{ref}}$ calculated over the spectral dimension.

$$\mathbf{x} = \frac{\mathbf{r}}{\overline{w}_{\text{ref}}}, \tag{8}$$

where $\mathbf{r}$ is the reduced-dimension spectrum. As can be seen from Figure 3, after pretreatment there is still a considerable amount of variation in the overall intensity of the spectra. Thus, the nonuniform illumination was only responsible for a small part of the overall variation in the reflectance levels, and a significant contribution is likely due to specular reflections from the faces of mineral crystals.

3.2 Cluster analysis

A principal component analysis (PCA) was carried out first, using the whole modelling data set. The objective was to find the spectral features which distinguish ore samples from gangue, and to compare different preprocessing methods. The following preprocessing methods were included in the analysis: no preprocessing, autoscaling, second difference, MSC and autoscaling, logarithmic transform, and logarithmic transform with second difference. A PCA model was estimated for each of the methods used, and the scores of these models, presented in Figure 4, were then examined to determine whether clustering of the data points in the principal component subspace corresponded to the classification of the samples.

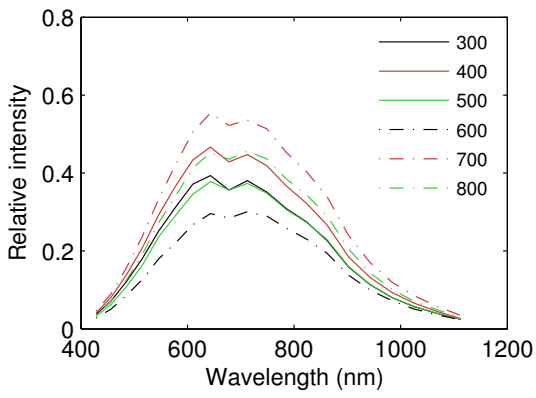

Fig. 3. Pretreated example spectra (cf. Fig. 2).

Clearly the used preprocessing method considerably affects the amount of clustering that can be observed in the principal component directions (Figure 4). The second difference, MSC and autoscaling, and the combined logarithmic transform and second difference all seem to be good preprocessing choices with regard to clustering. In all three the gangue samples are clearly separated from the ore samples. Among the alternatives MSC has the unique ability to cause sample A (the sole sample containing a significant amount of sphalerite) to be clearly presented as a cluster of its own. However, one of the ore data points has been projected to the gangue cluster.

If no preprocessing is used, the first principal component describes the data mean, and varies depending on the overall intensity of the spectrum. The separation according to sample type is primarily seen in the second principal component direction. Autoscaling seems to have a detrimental effect on the clustering, as the variation within the classes seems to have increased without an increase in the distance between the class cluster centers. The logarithmic transform alone is obviously the worst choice of the preprocessing methods, as it seems to increase the overlap between ore and gangue when compared to the model estimated with no preprocessing. Additionally, the clustering in this case was observed among the second and third principal components, and not among the first two as with the other preprocessing methods.

The clustering observed in the scores plot should also be compared to the mineral contents listed in Table 1. In this way the principal components can be related to the sample properties. For example, when the second difference is used as part of the data preprocessing (Figures 4(c) and 4(f)), it seems that the second principal component describes the amount of pyrite in the sample (samples A and E contain approximately 50 % pyrite, while samples F, M and N contain a low amount and the rest of the samples a high amount). Variation in the direction of the first principal component, on the other hand, does not seem to be related to the mineral contents.

3.3 Classification model

PLS-DA classification models were developed with the estimation data set. The same preprocessing methods as with PCA were used for comparison, and three additional methods (first difference, logarithmic transform and first difference, and pure MSC) were also included. Crossvalidation was used in model calibration, with 20 % of the data points randomly selected and not used in estimating the model parameters. The predictive ability of the models was then tested with the validation data set. The resulting classification errors and the root mean squared errors (RMSE) in calibration and in prediction are presented in Table 2, with the best RMSE and prediction error values in bold.

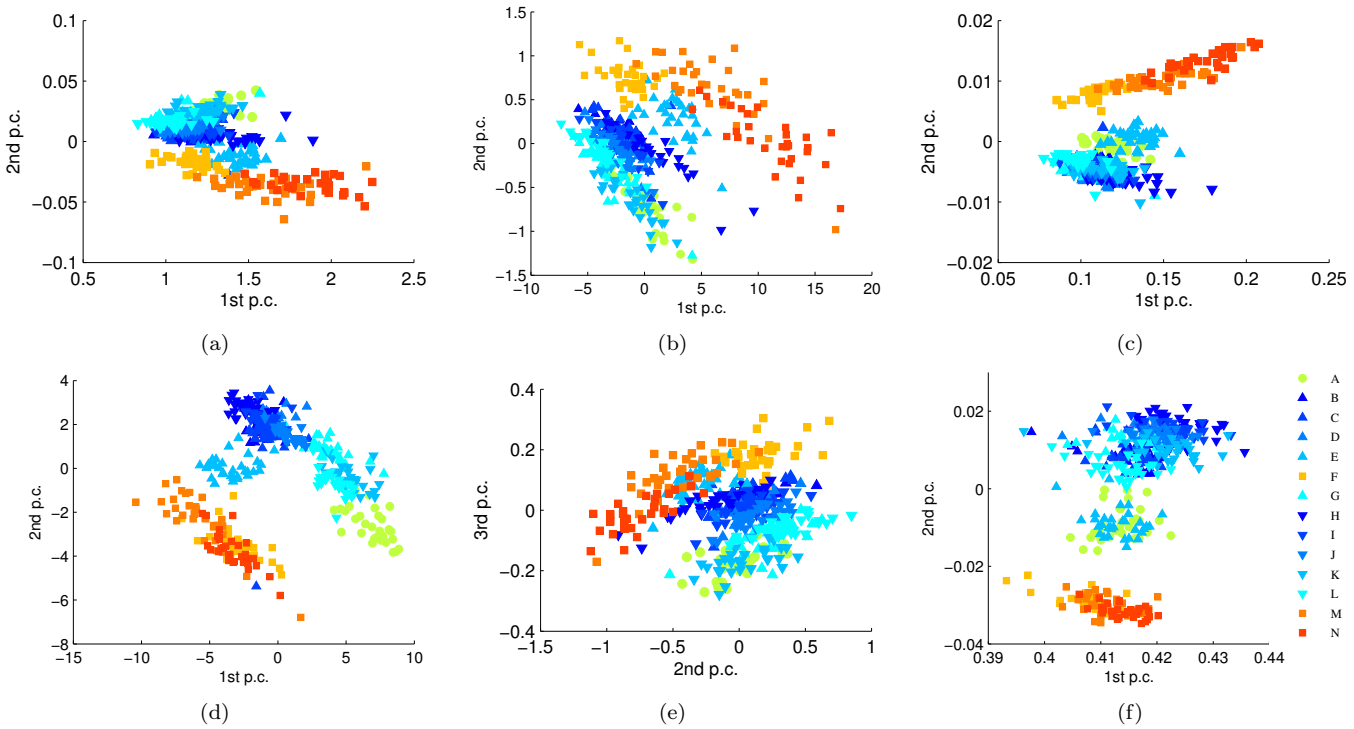

Fig. 4. Scores of some of the PCA models estimated with different preprocessing methods. The legend refers to the rock sample in which each of the data points belongs to. (a) No preprocessing, (b) Autoscaling, (c) 2nd difference, (d) MSC and autoscaling, (e) Logarithmic transform, (f) Logarithmic transform and second difference.

Table 2. Comparison of the classification error with different preprocessing methods

		Classification error			RMSE	
	Model order	calibration	crossvalidation	prediction	calibration	prediction
No preprocessing	2	0	0	0.064	0.131	0.245
Autoscaling	2	0	0	0.131	0.119	0.274
1st difference	2	0	0	0.025	0.097	0.192
2nd difference	2	0	0	**0**	0.120	**0.157**
logarithm	3	0.008	0.008	0.400	0.192	0.381
logarithm and 1st difference	2	0	0	0.055	0.116	0.234
logarithm and 2nd difference	3	0	0	0.053	0.081	0.209
MSC	3	0	0	0.041	0.076	0.207
MSC and autoscaling	3	0	0	0.045	**0.064**	0.208

The number of latent variables (model order) used in the model was selected based on the classification error and the amount of variance captured in the input data and the response variables. Based on the calibration and crossvalidation errors and the calibration RMSE, the best classification results were obtained using MSC with autoscaling as the preprocessing method. Good results were also achieved with taking the difference of the spectra once, or using the logarithmic transform and taking the difference twice. The worst classification performance was encountered with the logarithmic transform alone. These results are consistent with the PCA results.

For a reliable assesment of the classification models, the classification error and RMSE in prediction should be considered. A perfect classification result was achieved with the model where the second difference of the spectra was used as the input. The lowest RMSE was also encountered with this preprocessing method, and furthermore the second difference is the only alternative where only a modest increase in RMSE between calibration and prediction is seen. Again the logarithmic transform without further preprocessing has the worst performance, with rest of the alternatives roughly equal at least with regard to the RMSE. It is notable that autoscaling, often the default preprocessing choice with statistical multivariate methods, here increases the classification error and RMSE when compared with no preprocessing.

3.4 Test classification

The classification model which used the second difference as a preprocessing method was also tested with an additional test data set. The test data set was constructed by measuring the spectra of nine pieces of gangue rock from samples M and N laid on top of ore from sample G (Figure 5(a)). The test data set consisted of $32 \times 1280 = 40960$ single spectral measurements, unlike the estimation and

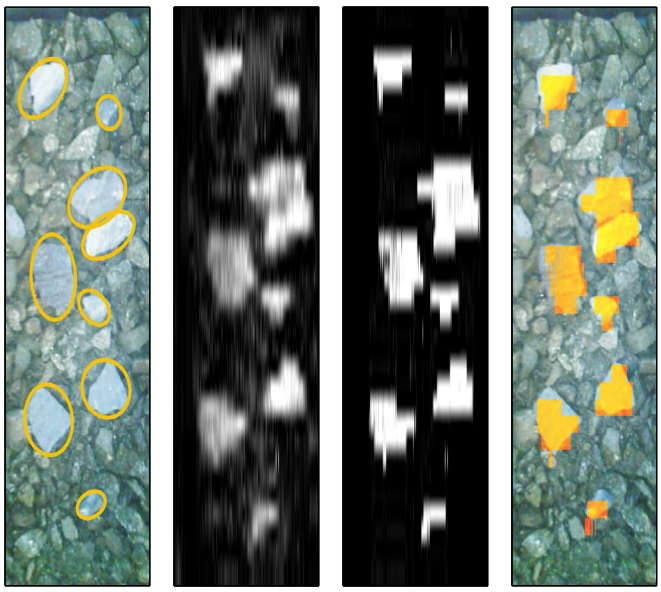

(a) (b) (c) (d)

Fig. 5. Classification results of the test set. (a) Image of the test sample (the pieces of gangue are circled). The image was taken with a conventional digital camera. (b) Output of the PLS-DA model. White areas indicate gangue. (c) Classification result after thresholding. (d) Classification result overlaid on the image of the test set.

validation data sets, which contained averaged spectra. The test set therefore presents a more demanding test of the classification performance of the model, since there is more noise in the input data than in the averaged validation data. The output of the classification model is shown in Figure 5(b) and the resulting classification after comparing the output with the threshold value in Figure 5(c). The contrast is high even in the output before thresholding, indicating a large separation between ore and gangue and therefore a robust classification result.

The performance of the classifier can be visually evaluated by overlaying the classification result on the image of the test sample (Figure 5(d)). All the pieces of gangue are correctly detected by the classification model. Only a fractional number of measurements seem to be misclassified, and these do not pose a problem to identifying the rock pieces in the sample. It can be concluded that even though the classifier was developed using the average spectra, it performs well also with individual spectra as inputs.

4. CONCLUSION

VNIR reflectance spectra were measured in laboratory conditions from rock samples whose mineral content was known. The spectrum measurements were subjected to different preprocessing methods and analyzed with PCA. It was observed that the clustering of measurement data clearly corresponded to ore type, and thus the VNIR spectrum was shown to be a viable measurement alternative for classifying rock samples. Partial least squared discriminant analysis (PLS-DA) models for determining the ore type were then developed, and validated with independent data. The final model demonstrated excellent performance and robustness in identifying the rock samples of a separate test data set.

In the future, the spectrum measurement and classification will be implemented in an actual mining environment for further study and online use. The measurement will also be combined with the ore particle size measurement already in operation.

REFERENCES

Barker, M. and Rayens, W. (2003). Partial least squares for discrimination. *Journal of Chemometrics*, 17, 166–173.

Basilevsky, A. (1994). *Statistical Factor Analysis and Related Methods*. John Wiley & Sons, Inc.

Borsaru, M., Zhou, B., Aizawa, T., Karashima, H., and Hashimoto, T. (2006). Automated lithology prediction from PGNAA and other geophysical logs. *Applied Radiation and Isotopes*, 64, 272–282.

Burns, D.A. and Ciurczak, E.W. (2008). *Handbook of Near-Infrared Analysis*. CRC Press, Boca Raton, Florida, third edition.

Casali, A., Gonzalez, G., Vallebuona, G., Perez, C., and Vargas, R. (2001). Grindability soft-sensors based on lithological composition and on-line measurements. *Minerals Engineering*, 14(7), 689–700.

Cutmore, N.G., Liu, Y., and Middleton, A.G. (1998). On-line ore characterisation and sorting. *Minerals Engineering*, 11(9), 843–847.

Geladi, P., MacDougall, D., and Martens, H. (1985). Linearization and scatter-correction for near-infrared reflectance spectra of meat. *Applied Spectroscopy*, 39(3), 491–500.

Gemperline, P. (ed.) (2006). *Practical guide to chemometrics*. CRC Press, Boca Raton, Florida, second edition.

Goetz, A.F.H., Curtiss, B., and Shiley, D.A. (2009). Rapid gangue mineral concentration measurement over conveyors by NIR reflectance spectroscopy. *Minerals Engineering*, 22, 490–499.

Guyot, O., Monredon, T., LaRosa, D., and Broussaud, A. (2004). VisioRock, and integrated vision techonology for advanced control of comminution circuits. *Minerals Engineering*, 17, 1227–1235.

Jackson, J.E. (2003). *A User's Guide to Principal Components*. John Wiley & Sons, Inc., Hoboken, New Jersey.

Kaartinen, J. and Tolonen, A. (2008). Utilizing 3D height measurement in particle size analysis. In *Proceedings of the 17th IFAC World Congress*.

Kaski, S., Häkkänen, H., and Korppi-Tommola, J. (2003). Sulfide mineral identification using laser-induced plasma spectroscopy. *Minerals Engineering*, 16, 1239–1243.

Singh, V. and Rao, S.M. (2005). Application of image processing and radial basis neural network techniques for ore sorting and ore classification. *Minerals Engineering*, 18, 1412–1420.

Sokolov, A.D., Docenko, D., Bliakher, E., Shirokobrod, O., and Koskinen, J. (2005). On-line analysis of chrome-iron ores on a conveyor belt using x-ray fluorescence analysis. *X-ray Spectrometry*, 34, 456–459.

Tessier, J., Duchesne, C., and Bartolacci, G. (2007). A machine vision approach to on-line estimation of run-of-mine ore composition on conveyor belts. *Minerals Engineering*, 20, 1129–1144.